Citation: CPT Pharmacometrics Syst. Pharmacol. (2015) 4, e22; doi:10.1002/psp4.22

ORIGINAL ARTICLE

Systems Pharmacology Approach Toward the Design of Inhaled Formulations of Rifampicin and Isoniazid for Treatment of Tuberculosis

NA Cilfone[1], E Pienaar[1,2], GM Thurber[1], DE Kirschner[2] and JJ Linderman[1]*

Conventional oral therapies for the treatment of tuberculosis are limited by poor antibiotic distribution in granulomas, which contributes to lengthy treatment regimens and inadequate bacterial sterilization. Inhaled formulations are a promising strategy to increase antibiotic efficacy and reduce dose frequency. We develop a multiscale computational approach that accounts for simultaneous dynamics of a lung granuloma, carrier release kinetics, pharmacokinetics, and pharmacodynamics. Using this computational platform, we predict that a rationally designed inhaled formulation of isoniazid given at a significantly reduced dose frequency has better sterilizing capabilities and reduced toxicity than the current oral regimen. Furthermore, we predict that inhaled formulations of rifampicin require unrealistic carrier antibiotic loadings that lead to early toxicity concerns. Lastly, we predict that targeting carriers to macrophages has limited effects on treatment efficacy. Our platform can be extended to account for additional antibiotics and provides a new tool for rapidly prototyping the efficacy of inhaled formulations.
CPT Pharmacometrics Syst. Pharmacol. (2015) **4**, e22; doi:10.1002/psp4.22; published online on 11 March 2015.

Tuberculosis (TB), caused by inhalation of the bacterium *Mycobacterium tuberculosis* (*Mtb*), remains a widespread concern even with the availability of curative antibiotics.[1–3] Current antibiotic regimens require a minimum of 6 months of treatment: daily oral doses with a combination of rifampicin (RIF), isoniazid (INH), pyrazinamide, and ethambutol for 2 months, followed by 4 months of RIF and INH.[4] The length and combinatorial nature of "first-line" drug regimens may result in patient compliance issues and chronic toxicity.[1,2,5] There is a desperate need for new strategies that can shorten lengthy treatment periods and reduce dose frequency.[1,5,6]

A central feature of the immune response to *Mtb* is the formation of granulomas, organized structures of macrophages and lymphocytes that form around infected macrophages and extracellular *Mtb* in lungs.[1,3,7] Multiple independently evolving granulomas form in a host's lungs.[8,9] The heterogeneity of *Mtb* populations in granulomas, with bacteria residing in both intra- and extracellular compartments, and varying growth states all influence the effectiveness of antibiotics.[1,10] Current oral antibiotic regimens can lead to poor antibiotic penetration into granulomas, causing suboptimal exposure, permitting bacterial re-growth between doses, and necessitating long treatment durations.[1,10,11]

Delivery of antibiotics by an inhaled route could overcome limitations of oral dosing for treatment of TB.[2,12–14] The principle of inhaled formulations is that a fabricated carrier loaded with antibiotics is dosed into the lungs by means of an aerosol delivery system (e.g., nebulizer).[13,14] Based on physical characteristics, carriers settle in different lung regions and are taken up by alveolar macrophages and lung endothelial cells.[2,12] Carriers release preloaded antibiotics based on tunable physiochemical properties such as carrier size and diffusivity of antibiotics through the carrier. The most extensively used carriers are poly-lactic acid (PLA) and poly-lactic-co-glycolic acid (PLGA) formulations that are tuned for slow and sustained release of antibiotics.[2,12] As granulomas are found in host lungs, an inhaled dose should elevate antibiotic concentrations in the lungs and avoid "first-pass" effects, thus increasing sterilizing capabilities. Additionally, targeting carriers to macrophages might further augment sterilizing capabilities of antibiotics by directly elevating concentrations within the bacterial niche.[12,13,15–18] With increased sterilizing capabilities, dosing frequency could be reduced, alleviating compliance and toxicity concerns associated with daily oral treatments.

Encapsulated formulations are rapidly phagocytosed by infected macrophages *in vitro,* elevating intracellular concentrations and improving sterilization capabilities.[15–17,19–21] However, these studies do not reflect the dense macrophage-laden characteristics of granulomas. Improved efficacy of inhaled doses compared with oral doses has been demonstrated in murine, rat, and guinea pig models of *Mtb* infection.[2,12–14,22,23] Although these studies have shed light on the efficacy of inhaled formulations, murine, rat, and guinea pig models have different antibiotic pharmacokinetics and lack many characteristics of human TB, such as latent infection and granuloma organization.[7,13] Relevant *in vivo* studies include single doses of inhaled formulations into the lungs of healthy nonhuman primates (INH) and humans (capreomycin).[24,25] An inhaled formulation of INH had twofold higher area-under-curve (AUC)/minimum-inhibitory-concentration (MIC) indices measured from plasma, compared with oral doses.[24] An inhaled

[1]Department of Chemical Engineering, University of Michigan, Ann Arbor, Michigan, USA; [2]Department of Microbiology and Immunology, University of Michigan Medical School, Ann Arbor, Michigan, USA. *Correspondence: JJ Linderman (linderma@umich.edu)
Received 13 June 2014; accepted 27 January 2015; published online on 11 March 2015. doi:10.1002/psp4.22

formulation of capreomycin leads to plasma concentrations above MIC, but for less than 4 h.[25] Although promising, most relevant *in vivo* studies are only able to measure temporal plasma concentrations after inhaled dosing. For inhaled formulations, it is assumed that extended periods of elevated antibiotic concentrations in plasma directly translate to increased exposure in granulomas.[1,19,24–27] However, oral dosing studies demonstrate that antibiotic exposure in granulomas is significantly different than antibiotic exposure in plasma.[1,10,11]

To better understand the potential for inhaled antibiotic formulations to improve sterilization of bacteria in granulomas, we need an approach that simultaneously accounts for granuloma dynamics, inhaled carrier behavior, release kinetics, pharmacokinetics, and pharmacodynamics of antibiotics. We use a systems pharmacology approach and extend our existing computational model of granuloma function and oral antibiotic treatment, from Pienaar *et al.*,[11] to include inhaled dosing and antibiotic release from a generalized carrier system. We follow concentrations of RIF and INH in granulomas for both inhaled and oral dosing to understand the effects of carrier physiochemical properties and release kinetics (e.g., size, diffusivity, etc.), dosing frequency, and pharmacokinetics on treatment efficacy. Using understanding gained from these studies, we rationally design inhaled formulations of RIF and INH given at reduced dose frequencies with equivalent or better sterilizing capabilities compared with daily oral dosing. These findings illuminate fundamental mechanisms driving efficacy of inhaled formulations and inform design of superior carriers for *in vivo* testing.

METHODS

Pharmacokinetic (PK) model. The four-components of our model are shown in **Figure 1**. We modify the PK model from Pienaar *et al.* to allow for dosing by means of both inhaled and oral routes.[11] The PK model (Eqs. 1–6) includes two transit compartments (C_{A1}, C_{A2}), a plasma compartment (C_{PL}), a peripheral compartment (C_{PE}), a noninfected lung compartment (C_L), an intracellular macrophage subcompartment (C_M) at pseudo-steady-state, and a granuloma compartment (described below) (**Figure 1a**).

$$\frac{dC_{A1}}{dt} = -K_A \cdot C_{A1} \quad \text{(Eq. 1)}$$

$$\frac{dC_{A2}}{dt} = K_A \cdot C_{A1} - K_A \cdot C_{A2} - CL_A \cdot C_{A2} \quad \text{(Eq. 2)}$$

$$\frac{dC_{PL}}{dt} = K_A \cdot C_{A2} - Q_P\left(\frac{C_{PL}}{V_{PL}} - \frac{C_{PE}}{V_{PE}}\right) - Q_L\left(PC_L \cdot \frac{C_{PL}}{V_{PL}} - \frac{C_L}{V_L}\right) \quad \text{(Eq. 3)}$$

$$\frac{dC_{PE}}{dt} = Q_P\left(\frac{C_{PL}}{V_{PL}} - \frac{C_{PE}}{V_{PE}}\right) - CL_{PE} \cdot \frac{C_{PE}}{V_{PE}} \quad \text{(Eq. 4)}$$

$$\frac{dC_L}{dt} = Q_L\left(PC_L \cdot \frac{C_{PL}}{V_{PL}} - \frac{C_L}{V_L}\right) + \sum_{N_{Ext}(t)}\left(M_{DL}(t)\left(\frac{V_L}{L_L}\right)\right) \quad \text{(Eq. 5)}$$

$$\frac{dC_M}{dt} = \sum_{N_{Int}(t)}\left(M_{DM}(t)(N_M \cdot L_M)\right) - CL_M \cdot C_M \quad \text{(Eq. 6)}$$

K_A is absorption rate (h^{-1}); CL_A, CL_{PE}, CL_M are clearance rate constants (L/kg*h) from second transit, peripheral, and macrophage compartments; Q_P and Q_L are between compartment transfer rate constants (h^{-1}); V_{PL}, V_{PE}, and V_L are apparent distribution volumes (L/kg) of plasma, peripheral, and noninfected lung compartments; PC_L is permeability coefficient for noninfected lung compartment; $M_{DL}(t)$ and $M_{DM}(t)$ are time-varying antibiotic release rates (mg/h) from inhaled carriers (described in Inhaled Carrier Model below); N_{Ext} and N_{Int} are time-varying number of inhaled carriers in noninfected lung and macrophage compartments; L_L is total lung volume (L), and N_M is number of macrophages in noninfected lung. The pseudo-steady-state between noninfected lung and intracellular macrophage compartments is given by:

$$C_L = \frac{A_T}{L_L + E_M \cdot N_M \cdot L_M} \quad \text{(Eq. 7)}$$

$$C_M = E_M \cdot C_L \quad \text{(Eq. 8)}$$

A_T is total mass (mg) of antibiotics (sum of intra- and extracellular); E_M is equilibrium partition coefficient, and L_M is volume (ml) of a macrophage. Antibiotics exit the plasma compartment and enter the granuloma compartment at vascular sources designated in the simulation grid (**Figure 1b**) based on the concentration gradients between the plasma compartment and the granuloma compartment (C_{Ext}).[11,28]

$$\frac{dC_{Ext}(x,y,t)}{dt} = (p \cdot A_S)\left(PC_L \cdot C_{PL} - C_{Ext}(x,y,t)\right) \quad \text{(Eq. 9)}$$

A_S is surface area of a vascular source (cm^2), P is vascular permeability (cm/s), and PC_L is partition coefficient. PK model parameters are given in **Supplementary Table S1**.

Granuloma model of *Mtb* infection. Our two-dimensional hybrid multiscale agent-based model of granuloma formation and function during *Mtb* infection describes processes across three scales: tissue, cellular, and molecular (**Figure 1b**; **Supplementary Model Appendix S1**).[11,29–32] Briefly, the granuloma model represents a 16 mm^2 section of lung tissue and describes macrophages, T-cells, and three *Mtb* subpopulations: intracellular, extracellular, and nonreplicating. The formation of a granuloma is an emergent behavior in response to infection. The model tracks agent states, interactions, and chemokine/cytokine diffusion and degradation. Receptor-ligand trafficking and signaling events are estimated using a tuneable resolution approach.[11,29,31,33] The model captures spatial and temporal dynamics of RIF and INH through extracellular diffusion and degradation, cellular uptake and intracellular degradation.[11] Cellular accumulation of soluble antibiotics is assumed at pseudo-steady-state given by:

$$C_{Ext}(x,y,t) = \frac{A_T(x,y,t)}{L_{Grid} + E_M \cdot L_M} \quad \text{(Eq. 10)}$$

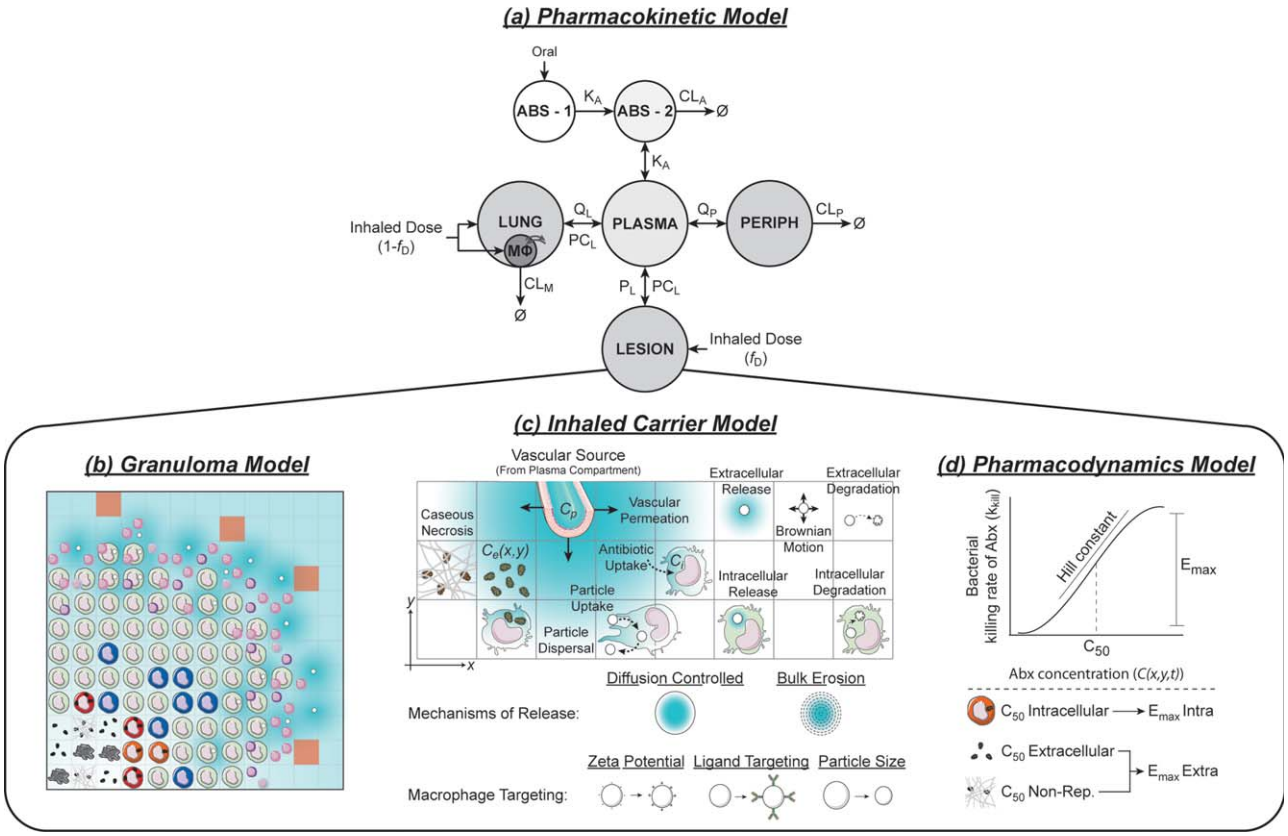

Figure 1 Overall model structure that captures relevant dynamics across multiple compartments. **(a)** The pharmacokinetic (PK) model includes two transit compartments (*ABS-1* and *ABS-2*) which approximate gut absorption and transit time, a plasma compartment (*PLASMA*), a peripheral compartment (*PERIPH*), a noninfected lung compartment (*LUNG*), and an intracellular macrophage compartment (*MΦ*) that is at pseudo-steady-state. Oral doses enter into the first transit compartment. Inhaled doses are partitioned between the noninfected lung (1-f_D) and lesion (f_D) models based on representative sizes. The dose (1-f_D) into the noninfected lung compartment is further partitioned between extracellular noninfected lung and intracellular macrophage compartments. We assume no trafficking of macrophages in or out of noninfected lungs. **(b)** Our granuloma model, a hybrid multiscale agent-based model, includes spatial and temporal dynamics of antibiotics and captures diffusion, extracellular degradation, cellular uptake and intracellular degradation. Antibiotics exit the plasma compartment and enter the granuloma model at vascular sources designated in the simulation grid based on vascular permeability coefficients and concentration gradients between the plasma compartment and the granuloma mode. The inhaled formulation is modeled by agent representations of each carrier. **(c)** Model of the behavior and release of antibiotics by inhaled carriers. Carriers move by random walk, are phagocytosed by macrophages based on size, zeta potential, and density of targeting ligand (**Supplementary Figure S1b-d**), degrade in both the extra- and intracellular space, and release antibiotics in both the intra- and extracellular space. **(d)** The pharmacodynamics model uses E_{max} functions (using C_{50} values and Hill-constants, H) to describe the antibacterial activity of antibiotics against multiple bacterial subpopulations (intracellular, extracellular, and nonreplicating) based on the local antibiotic concentration ($C(x,y,t)$). Art adapted from Servier Medical Art (http://servier.com/Powerpoint-image-bank) provided under the Creative Commons Unported License 3.0.

$$C_{Int}(x,y,t) = E_M \cdot C_{Ext}(x,y,t) \qquad \text{(Eq. 11)}$$

C_{Ext} and C_{Int} are extra- and intracellular concentrations (mg/ml), and L_{Grid} is volume (ml) of a grid compartment. Parameter values for apparent RIF and INH diffusivity (cm^2/s), intra- and extracellular degradation rate (s^{-1}), and equilibrium partition coefficient were fit to experimental measurements of antibiotic distribution in Pienaar *et al*.[11] Granuloma model parameters are given in **Supplementary Table S2**.

Inhaled carrier model: granuloma compartment. An inhaled dose arrives in the granuloma model, as fraction f_D of the total dose (**Figure 1a**). The granuloma model represents a small section of lung tissue where infection occurs, and individual carriers ($\sim 10^3$ deposited carriers) are modeled as agents (**Figure 1c**). We assume the representative section of lung tissue contains ample alveolar space, and thus an inhaled dose is randomly deposited into the simulation environment. Deposition does not occur in microcompartments characterized as part of the granuloma, as alveolar space is not observed inside granulomas (**Supplementary Figure S1a**).[9,34] We do not model specific carriers, but instead describe a general carrier formulation similar to polymer-encapsulated antibiotics.[15–17,19–21] Carrier behavior is illustrated in **Figure 1c** and includes carrier movement, macrophage phagocytosis of carriers (**Supplementary Figure S1b-d**), dispersal from macrophages, and extra- and intracellular degradation.[18,35–39]

Release of antibiotics from carriers occurs in both the intra- and extracellular environment (**Figure 1c**).[15–17,19–21] We model release kinetics by describing diffusion of antibiotics through a spherical carrier and degradation of the carrier system itself, with time varying boundary conditions.[40–42]

$$\frac{\partial C_D}{\partial t} = \frac{D(t)}{r^2}\frac{\partial}{\partial r} r^2 \frac{\partial C_D}{\partial r} \qquad C_D(R) = C_B(x, y, t) \qquad \text{(Eq. 12)}$$

C_D is antibiotic concentration in the carrier (mg/μm^3), D is time-varying diffusivity of antibiotics in the carrier (μm^2/s), r is the radial coordinate (μm), R is carrier radius (μm), and C_B is the boundary concentration (mg/μm^3), an intra- or extracellular concentration. We assume first-order degradation kinetics, which directly affects diffusivity of antibiotics in carriers[41]:

$$D(t) = P_{drugDiff} e^{(-P_{deg} t)} \qquad \text{(Eq. 13)}$$

$P_{drugDiff}$ is the initial diffusivity of antibiotics in the carrier (μm^2/s) and P_{deg} is the carrier degradation rate (s^{-1}), specific to whether the carrier is intra- or extracellular. Based on relative rates of diffusion and degradation specified, carrier release kinetics can be either diffusion-controlled or degradation-controlled (**Figure 1c**).[40–42] All carrier parameters are given in Supplementary **Table S1**.

Inhaled carrier model: noninfected lung compartment. An inhaled dose arrives in the noninfected lung and intracellular macrophage compartments, as fraction *(1-f_D)* of the total dose (**Figure 1a**). The number of carriers deposited is large ($\sim$10^9) and a homogenous representation of carriers is used (**Figure 1a**). We partition the *(1-f_D)* dose into both compartments, based on the probability of macrophage uptake. We solve carrier release equations (Eqs. 12–13) for a representative carrier in each compartment with appropriate boundary conditions, C_L and C_M, and scale the mass of antibiotic release by the total dose in each compartment. Carrier degradation rates are set as the extracellular degradation rate for the noninfected lung compartment and the intracellular degradation rate for the intracellular macrophage compartment.

Pharmacodynamic (PD) model. We use a PD model (**Figure 1d**) calibrated against nonhuman primates (NHPs) given monotherapies of RIF or INH constructed in Pienaar *et al*.[11] Briefly, E_{max} functions (using C_{50} values and Hill-constants, H) describe the antibacterial activity of RIF and INH against multiple bacterial subpopulations (**Figure 1d**) based on the local antibiotic concentration (intra- or extracellular), which varies in both space and time in the granuloma model. Estimates of C_{50} and H were based on *in vitro* dose-response curves, while estimates of E_{max} were determined from comparisons to NHP data of colony forming units (CFU) and sterilized granulomas after 2 months of daily dosing with RIF or INH.[11,43] PD model parameters are given in Supplementary **Table S1**.

Model analysis

We investigate antibiotic efficacy at the single granuloma scale. We simulate 100 d postinfection and subsequently treat with antibiotics for an additional 200 d by means of the oral or inhaled route (two dosing frequencies: daily or every 2 weeks). We define successful granuloma treatment as sterilization of all bacteria in a granuloma by 200 d post-treatment initiation. NHPs have a range of 3–30 granulomas; the probability of successfully sterilizing all granulomas in a single NHP is significantly lower than on an individual granuloma scale. We calculate cumulative granuloma and peripheral antibiotic exposure (AUC) for 14-d timeframes. Peripheral AUC is used as an estimate of toxicity.[10] Uncertainty and sensitivity analysis is used to identify inhaled antibiotic model parameters that have significant effects on model outputs related to treatment efficacy.[44] Additional model details can be found in the **Supplementary Text**.

RESULTS

Model calibration with non-human primate experimental data

Our granuloma model of *Mtb* infection, without antibiotic treatment (**Figure 1b**), was previously calibrated and validated against measurements of CFU per granuloma from a NHP model of TB.[8,11,32] We calibrate our modified PK model (**Figure 1a**) with previously published data for two dose formulations from NHP models of TB (**Figure 2**): (1) oral doses of RIF (20 mg/kg) or INH (15 mg/kg), with plasma concentrations measured over 24 h (**Figure 2a,b**)[6]; (2) single inhaled dose of INH-loaded PLA microparticles, with plasma concentration measured over 24 h (**Figure 2c**).[8,24] Deposition of inhaled particles is influenced by physiochemical properties, inhalation methods, and variability in patient inhalation, impacting bioavailability and treatment efficacy.[45] We focus on processes downstream of inhalation and deposition, but future studies could include computational fluid dynamics-based models of human lung deposition.[45] Based on measured microparticle size, aerodynamic diameter, and fractional lung deposition ($\sim$10%–30%), we estimate the total deposited inhaled dose (input to our model) to be 1.2 $\times$ 10^9 particles.[24,46] We fix the deposited dose at this physiologically relevant value here and in all further simulations. Using the oral doses and calculated carrier-related parameters (**Figure 2**, legend), we vary multiple PK parameters to best fit plasma kinetics of single oral doses of RIF and INH and a single inhaled dose of INH (**Figure 2**).[6,18,24] We establish baseline ranges of PK-related parameters that account for host-to-host variability and randomly choose parameter values from these ranges (**Supplementary Text** and **Supplementary Table S1**).

Combination of pharmacokinetic and carrier-release properties control the efficacy of inhaled formulations

We use sensitivity analysis to understand which dynamics most affect treatment efficacy (CFU, granuloma AUC, peripheral AUC, and time to sterilization) for inhaled formulations of RIF and INH. We analyzed daily and 2-week dosing frequencies to compare changes in treatment dynamics at reduced frequencies. **Tables 1** and **2** demonstrate that:

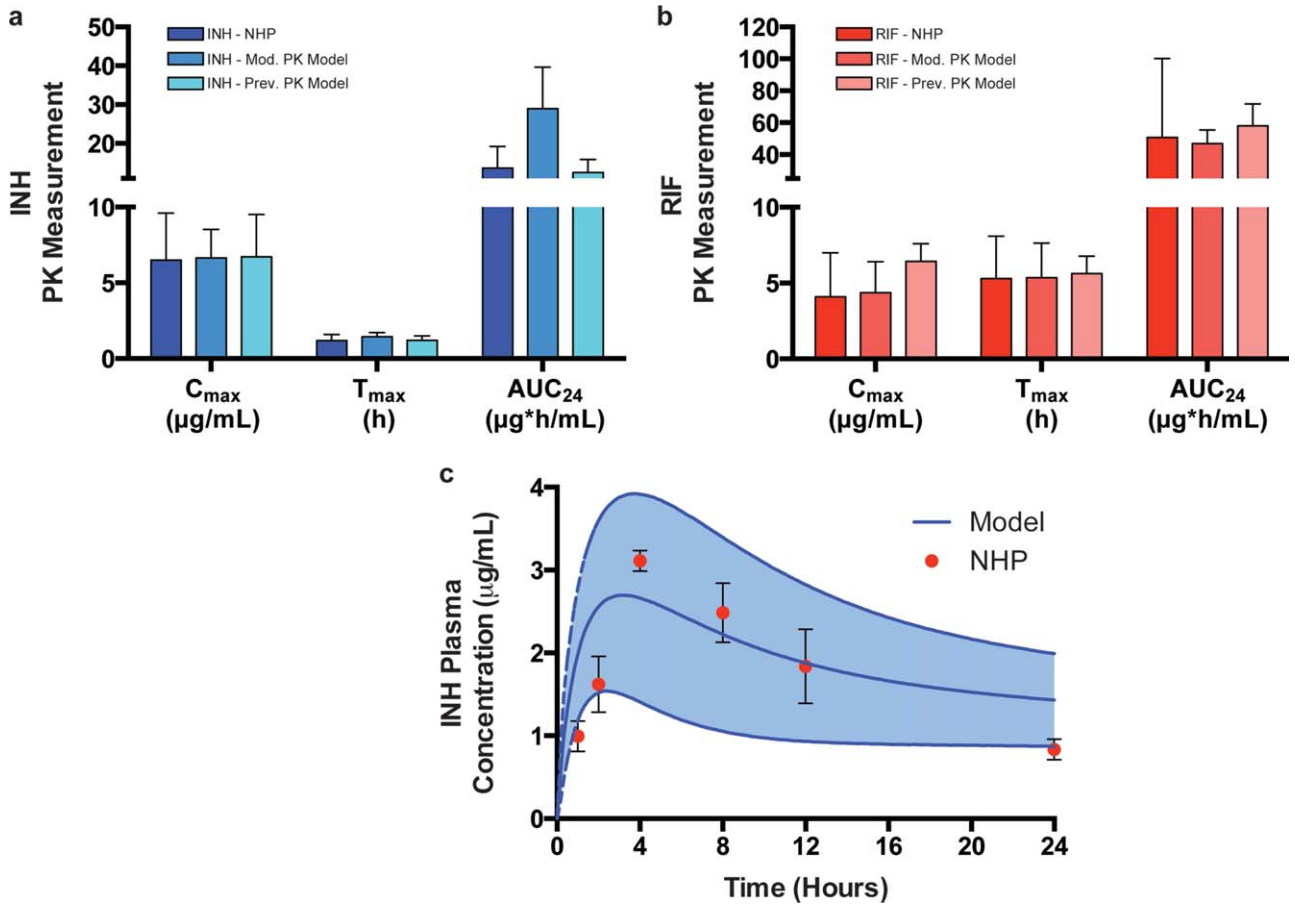

Figure 2 Model calibration and validation for oral and inhaled doses. **(a,b)** Comparison of the modified pharmacokinetic (PK) model (this work) and previous PK model (**Supplementary Text**) to maximum plasma concentration (C_{max}), time to maximum plasma concentration (T_{max}), and 24-h area under curve (AUC_{24}) for oral doses of rifampicin (RIF) and isoniazid (INH) in the nonhuman primate (NHP) model of TB published by the Flynn Lab (see Supplemental Information from Lin *et al*.[6] for concentration vs. time data).[6] Ranges are used for multiple model PK parameters (absorption rates, clearance rates, and volume of distributions – see **Supplementary Table S1**) to give inter-individual variability (based on ranges for RIF and INH derived from the NHP model in Lin *et al*.[6]). Bars are representative of mean values with error bars showing standard deviation (SD). Simulation replicates: $N = 50$, NHP: Experimental replicates $N = 7$. **(c)** Validation of the model against observed plasma concentrations of INH after single inhalation to healthy NHPs estimated from.[18,24] Dots represent mean experimental values with error bars showing SD. Line represents mean model values with dotted lines showing SD. Ranges are used for multiple model PK parameters to give inter-individual variability (absorption rates, clearance rates, and volume of distributions – see **Supplementary Table S1**). Model: $N = 10$, NHP: $N = 4$. Carrier-related parameters for the single inhaled dose were estimated based on data and Eqs. 12–13: $D = 1.85 \times 10^{-6}$ ($\mu m^2/s$), $\delta_c = 1.65 \times 10^{-5}$ (s^{-1}), and INH loading of 1.45×10^{-8} (mg/particle).[18]

(1) increased antibiotic loading promotes bacterial sterilization, (2) carrier release kinetics control treatment efficacy and differ with dosing frequency, and (3) pharmacokinetics influence availability of antibiotics in granulomas (**Supplementary Text** and **Supplementary Tables S3 and S4**).

For both RIF and INH, more frequent inhaled dosing (daily) allows carriers to be designed with faster carrier-release profiles (higher diffusivity in the carrier and degradation rates) as another dose is given after a short interval (**Tables 1** and **2**). Faster carrier release profiles are negatively correlated with CFU and time to sterilization, and positively correlated with granuloma and peripheral AUC. With less frequent dosing (every 2 weeks) INH requires a carrier designed with slower carrier-release and degradation profiles to maintain high levels of granuloma exposure with decreased CFU (**Table 2**). RIF requires a carrier designed with faster carrier-release profiles to increase granuloma exposure but this has limited effects on CFU (**Table 2**). Pharmacokinetic parameters have large influences on antibiotic exposure in granulomas for both dosing frequencies; clearance of RIF and INH from the peripheral compartment is correlated with many facets of treatment dynamics (**Tables 1** and **2**).

Targeting inhaled formulations to macrophages has limited effects on treatment efficacy due to the dynamics of granulomas

Targeting inhaled carriers to macrophages (the bacterial niche) could enhance efficacy of inhaled treatments, as phagocytosis of carriers *in vitro* leads to increased intracellular concentrations of antibiotics.[15–17,19–21] Yet, there is no direct evidence that targeting inhaled carriers to

Table 1 Sensitivity analysis of inhaled RIF model parameters at different dose frequencies on treatment related model outputs[a]

		Carrier release parameters					Mϕ targeting parameters							PK parameters			
	Rifampicin	P_{load}	P_{size}	$P_{drugDiff}$	P_{intDeg}	P_{extDeg}	P_{zeta}	P_{diff}	M_{uptake}	P_{TL}	M_{TR}	$K_{D\text{-}TLR}$	k_{TLR}	k_{abs}	CL_{abs}	V_p	CL_p
Daily	CFU	−−−	+	−−−	−												+
	Lesion AUC	+++	−−	+++	+++	+++	++	−	−−−		−						−−−
	Peripheral AUC	+++	−−−	+++	+++	+++										+++	−−−
	Time to sterilization	−−−		−−											−		+
2 weeks	CFU	−−−			+	+++											+
	Lesion AUC	+++		+++	++	+	+		−		+						−−−
	Peripheral AUC	+++		+		+				−						+++	−−−
	Time to sterilization	−−−															

P_{load}, load mass of drug (mg/carrier); P_{size}, size of carrier (μm); $P_{drugDiff}$, diffusivity of drug in carrier (μm^2/s); P_{intDeg}, carrier intracellular degradation rate (L/s); P_{extDeg}, carrier extracellular degradation rate (L/s); P_{zeta}, carrier zeta-potential (mV); P_{diff}, diffusivity of carrier in lung tissue (cm^2/s); M_{uptake}, macrophage maximum carrier uptake probability (unitless); P_{TL}, carrier density of targeting ligand (#/carrier); M_{TR}, macrophage density of targeting receptor (#/cell); $K_{D\text{-}TLR}$, ligand-receptor dissociation constant (M); k_{TLR}, ligand-receptor carrier uptake rate (#/cell*s); k_{abs}, absorption rate constant (1/hr); CL_{abs}, clearance rate from the second absorption compartment (L/h*kg); CL_p, peripheral volume distribution (L/kg); V_p, peripheral volume distribution (L/kg); CL_p, clearance rate from peripheral compartment (L/h*kg); -/+, $P < 0.05$; --/++, $P < 0.001$; ---/+++, $P < 0.0001$ from sensitivity analysis.
[a]Carrier dose used: 1.2×10^9 carriers. +/- signs indicate positive or negative correlations. The number of +/- signs indicates the strength of correlations (e.g., +++ vs. + indicates a stronger positive correlation of the former parameter compared to the latter parameter).[43]

Table 2 Sensitivity analysis of inhaled INH model parameters at different dose frequencies on treatment related model outputs

		Carrier release parameters					Mϕ targeting parameters							PK parameters			
	Isoniazid	P_{load}	P_{size}	$P_{drugDiff}$	P_{intDeg}	P_{extDeg}	P_{zeta}	P_{diff}	M_{uptake}	P_{TL}	M_{TR}	$K_{D\text{-}TLR}$	k_{TLR}	k_{abs}	CL_{abs}	V_p	CL_p
Daily	CFU	−−−		−−−	−−		−										+++
	Lesion AUC	+++	−−	+++	+++	++											−−−
	Peripheral AUC	+++	−	+++	+++	++										+++	−−−
	Time to sterilization	−−−	+	−−−	−												+++
2 weeks	CFU	−−−	−	+	+									−			+++
	Lesion AUC	+++		+	+									+	−		−−−
	Peripheral AUC	+++		+										+		+++	−−−
	Time to sterilization	−−−															+++

P_{load}, load mass of drug (mg/carrier); P_{size}, size of carrier (μm); $P_{drugDiff}$, diffusivity of drug in carrier (μm^2/s); P_{intDeg}, carrier intracellular degradation rate (L/s); P_{extDeg}, carrier extracellular degradation rate (L/s); P_{zeta}, carrier zeta-potential (mV); P_{diff}, diffusivity of carrier in lung tissue (cm^2/s); M_{uptake}, macrophage maximum carrier uptake probability (unitless); P_{TL}, carrier density of targeting ligand (#/carrier); M_{TR}, macrophage density of targeting receptor (#/cell); $K_{D\text{-}TLR}$, ligand-receptor dissociation constant (M); k_{TLR}, ligand-receptor carrier uptake rate (#/cell*s); k_{abs}, absorption rate constant (L/h); CL_{abs}, clearance rate from second absorption compartment (L/h*kg); V_p, peripheral volume distribution (L/kg); CL_p, clearance rate from peripheral compartment (L/h*kg); -/+, $P < 0.05$; --/++, $P < 0.001$; ---/+++, $P < 0.0001$ from sensitivity analysis.
Carrier dose used: 1.2×10^9 carriers. +/- signs indicate positive or negative correlations. The number of +/- signs indicates the strength of correlations (e.g., +++ vs. + indicates a stronger positive correlation of the former parameter compared to the latter parameter).[43]

macrophages in granulomas provides any treatment advantage. Using sensitivity analysis we explored the effects of macrophage targeting on treatment efficacy (CFU, granuloma AUC, peripheral AUC, and time to sterilization) for inhaled formulations of RIF and INH. We varied parameters that control macrophage uptake including carrier charge, movement rate, and a generalized form of ligand targeting (**Tables 1** and **2**).

Our analysis predicts that parameters influencing targeting of inhaled carriers to macrophages have limited effects on treatment efficacy for both RIF and INH. At both dosing frequencies of inhaled formulations of RIF, increased macrophage targeting leads to decreased antibiotic exposure in granulomas and actually hinders sterilization of bacteria (**Table 1**). For daily dosing of an inhaled formulation of INH, increased carrier charge (causing decreased uptake) is negatively correlated with CFU (**Table 2**). Macrophage targeting is limited by granuloma structure as it prevents inhaled carriers from trafficking to, and being phacoytosed by, infected macrophages in the core of granulomas. This restricts any proposed advantages of elevated intracellular antibiotic concentrations. This limits macrophage uptake to outer region granulomas, where populations are mainly healthy macrophages (movies – http://malthus.micro.med.umich.edu/lab/movies/InhaledAbx/). Therefore, our model predicts that there are no significant treatment benefits in designing inhaled carriers that specifically target macrophages due to the spatial dynamics of granulomas.

An inhaled formulation of RIF can reduce the necessary dose frequency but requires high antibiotic loading which can lead to increased toxicity

We identified 14 different inhaled formulations of RIF, dosed every 2 weeks, from sensitivity analysis that had equivalent CFU and reduced peripheral AUC at 7 d posttreatment initiation compared with daily dosed oral formulations

a

	Dosing Method	
	Oral	*Inhaled*
Dose Frequency	Daily	2 Weeks
Single Dose (mg/kg)	20	280
Total 2 Week Dose (mg/kg)	280	280
Inhaled Carrier Properties		
Intracellular $t_{1/2}$ (h)	59.2	
Extracellular $t_{1/2}$ (h)	192.5	
Diffusivity in Carrier ($\mu m^2/s$)	$2x10^{-7}$	

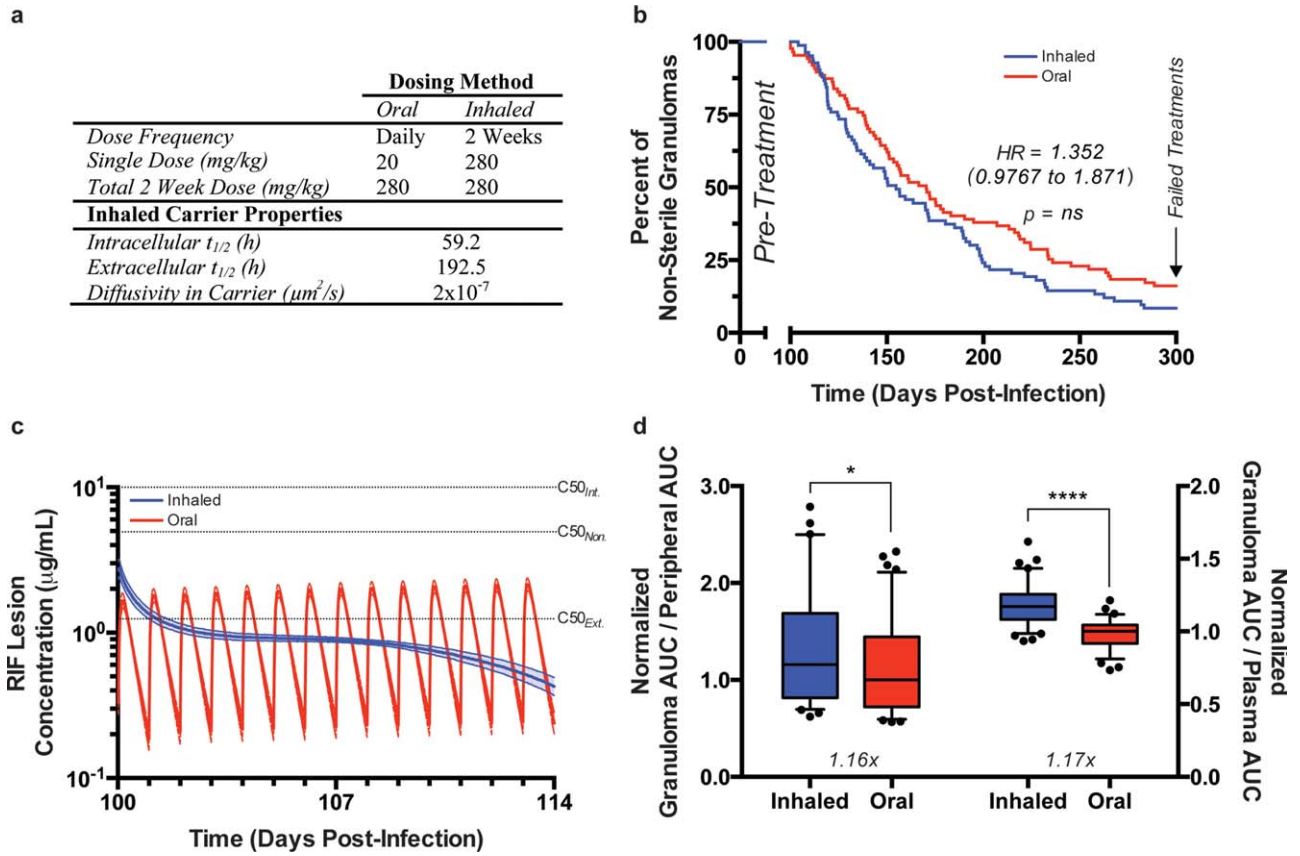

Figure 3 Comparison of an inhaled rifampicin (RIF) formulation given every 2 weeks with an oral RIF formulation given daily. **(a)** Comparison of the total 2-week dose between formulations for the given properties of the inhaled formulation. **(b)** Percent of granulomas not sterilized at indicated times after the initiation of treatment. Granulomas still present at 300 d postinfection are considered failed treatments. **(c)** Average RIF concentration in the granuloma for the first 14-d dosing window. Solid lines indicate average values while dotted lines represent standard deviation. Dotted black lines indicate $C50_{Int}$, $C50_{Non}$, $C50_{Ext}$ for RIF. Minimum inhibitory concentration (MIC) of RIF is between 0.03 and 0.5 μg/ml. **(d)** Granuloma area under curve (AUC)/Peripheral AUC and Granuloma AUC/Plasma AUC for the first 14-d dosing window. Values are normalized to the median value of the oral dosing. Box and whiskers represent the 5 to 95% range with data points outside the interval shown as black dots. $^*P \leq 0.05$, $^{**}P \leq 0.01$, $^{***}P \leq 0.001$, $^{****}P \leq 0.0001$. Inhaled simulation replicates ($N = 83$). Oral simulation replicates ($N = 87$). See movies at http://malthus.micro.med.umich.edu/lab/movies/InhaledAbx/

(**Supplementary Text**). Using these candidates along with an understanding of which dynamics most affect treatment efficacy, we designed an ideal *in silico* inhaled formulation of RIF dosed every 2 weeks. We design the carrier with a RIF loading of 1.18×10^{-6} mg/particle, an extracellular degradation rate threefold lower than the intracellular rate, and a high RIF carrier diffusivity, which promotes rapid-release of antibiotics from the carrier (**Figure 3a**); the total 2-week dose is equivalent to the oral formulation. We observed no significant difference between the inhaled formulation, given every 2 weeks, and daily oral dosing when comparing hazard ratios (HR) (**Figure 3b**). The inhaled formulation may prevent treatment failures by increasing early sterilizing capabilities of RIF compared with daily oral dosing (**Supplementary Figure S2a**).

Comparing average granuloma concentrations of RIF between the two formulations, we observe a significant difference in temporal dynamics: the inhaled formulation only eclipses the C_{50} of extracellular *Mtb* immediately after dosing and never surpasses the C_{50} for intracellular or nonreplicating *Mtb* (**Figure 3c**). Average granuloma concentrations of RIF steadily decrease, indicating that high antibiotic loading and fast carrier-release kinetics cannot maintain effective concentrations of RIF over the 2-week dosing window (**Figure 3c**) (movies – http://malthus.micro.med.umich.edu/lab/movies/InhaledAbx/). In part, this is due to the pharmacokinetics of RIF as it distributes rapidly from the site of dosing (lung) to other tissues, as demonstrated by the limited changes in the normalized ratio of granuloma to peripheral AUC (16%) and granuloma to plasma AUC (17%) (**Figure 3d**). Early granuloma and peripheral AUCs are elevated after inhaled dosing compared with oral dosing, indicating that early granuloma exposure is associated with elevated toxicity (**Supplementary Figure S2b-d**). Daily oral dosing has similar problems surpassing C_{50} values for intracellular and nonreplicating *Mtb*, but the higher dosing frequency leads to average granuloma concentrations that exceed the C_{50} of extracellular *Mtb* after each dose

a

	Dosing Method	
	Oral	*Inhaled*
Dose Frequency	Daily	2 Weeks
Single Dose (mg/kg)	15	17.1
Total 2 Week Dose (mg/kg)	210	17.1
Inhaled Carrier Properties		
Intracellular $t_{1/2}$ (h)	50.6	
Extracellular $t_{1/2}$ (h)	50.6	
Diffusivity in Carrier ($\mu m^2/s$)	5.8×10^{-8}	

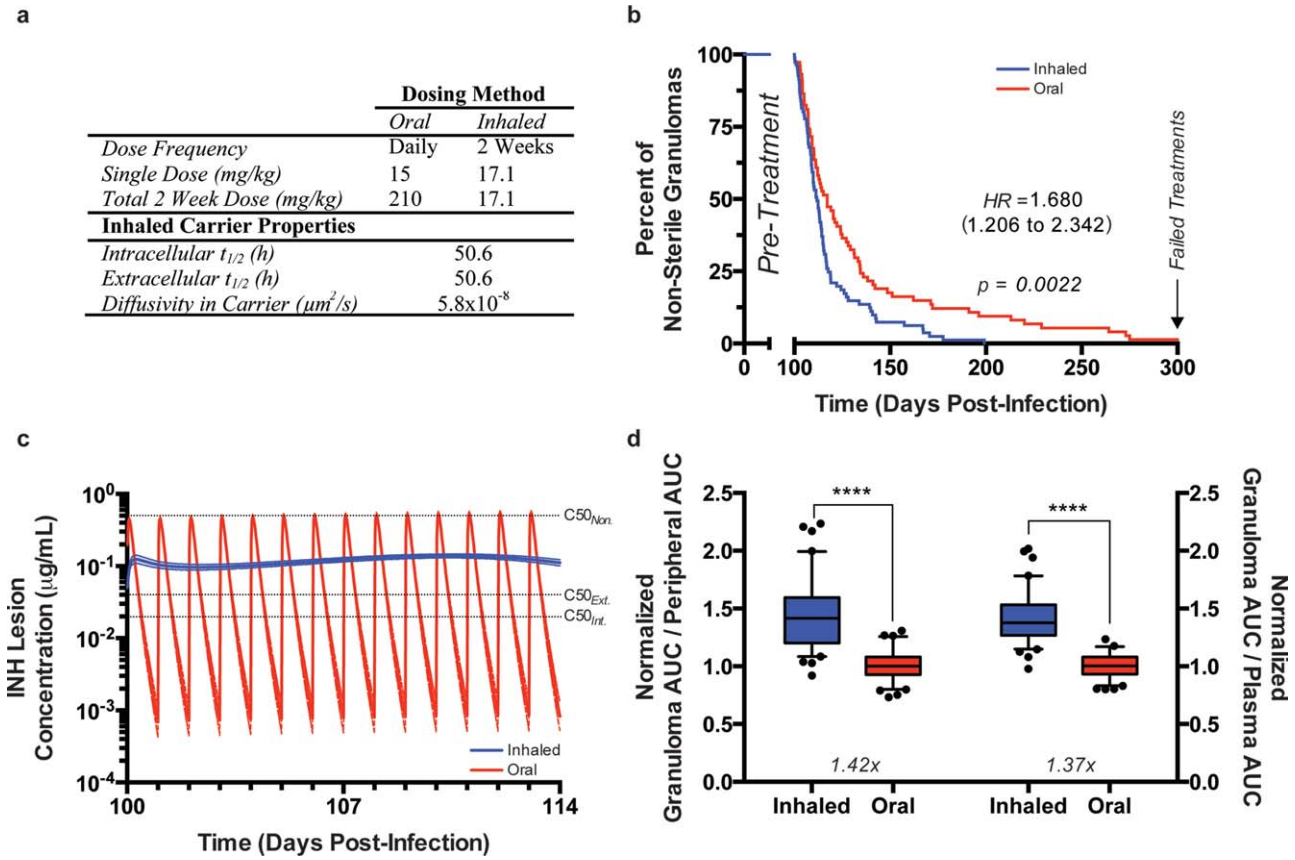

Figure 4 Comparison of an inhaled isoniazid (INH) formulation given every 2 weeks with an oral INH formulation given daily. **(a)** Comparison of the total 2-week dose between formulations for the given properties of the inhaled formulation. **(b)** Percent of granulomas not sterilized at indicated times after the initiation of treatment. Granulomas still present at 300 d postinfection are considered failed treatments. **(c)** Average INH concentration in the granuloma for the first 14-d dosing window. Solid lines indicate average values while dotted lines represent standard deviation. Dotted black lines indicate $C50_{Int}$, $C50_{Non}$, $C50_{Ext}$ for INH. Minimum inhibitory concentration (MIC) of INH is between 0.05 and 0.1 μg/ml. **(d)** Granuloma area under curve (AUC)/Peripheral AUC and Granuloma AUC/Plasma AUC for the first 14-d dosing window. Values are normalized to the median value of the oral dosing. Box and whiskers represent the 5 to 95 percentage range with data points outside the interval shown as black dots. $^{*}P \leq 0.05$, $^{**}P \leq 0.01$, $^{***}P \leq 0.001$, $^{****}P \leq 0.0001$. Inhaled simulation replicates ($N = 81$). Oral simulation replicates ($N = 87$). See movies at http://malthus.micro.med.umich.edu/lab/movies/InhaledAbx/.

(**Figure 3c**). Taken together, these results suggest that the dosing frequency of RIF could be reduced by appropriately designing an inhaled formulation. However, there is increased early toxicity, a possibility in reducing RIF to a bacteriostatic agent due to low concentrations within granulomas, and limited feasibility based on the high carrier loading that would be required.

An inhaled formulation of INH can reduce the necessary dose frequency, increase therapeutic efficacy, and lessen toxicity

We identified eight different inhaled formulations of INH, dosed every 2 weeks, from sensitivity analysis that had equivalent or reduced CFU and reduced peripheral AUC at 7 d posttreatment initiation compared with daily dosed oral formulations (**Supplementary Text**). Using these candidates, along with an understanding of which dynamics most affect treatment efficacy, we designed an ideal *in silico* inhaled formulation of INH to be dosed every 2 weeks. Based on the parameter values of candidate formulations, we design the carrier with an INH loading of 7.2×10^{-8} mg/particle, a similar intra- and extracellular degradation rate, and a low INH carrier diffusivity, causing slow-release of antibiotics from the carrier (**Figure 4a**). This equates to a 12-fold lower total 2-week dose compared with the oral formulation. We observe a significant difference in sterilizing capabilities between the inhaled formulation, given every 2 weeks, and daily oral dosing (**Figure 4b**). The HR is 1.6 (95% confidence interval: 1.2 to 2.3) demonstrating decreased time to sterilization (all sterilized by 100 d post-treatment) and fewer failed treatments with an inhaled formulation (**Figure 4b**).

Average INH granuloma concentrations during treatment with the inhaled formulation are sustained above C_{50} values for intra- and extracellular *Mtb* populations for the entire dosing window, compared with daily oral dosing (**Figure 4c**) (movies – http://malthus.micro.med.umich.edu/lab/movies/InhaledAbx/). Sustained granuloma concentrations of INH during treatment prevent bacterial re-growth between doses associated with daily oral INH dosing

(**Supplementary Figure S3a**). The inhaled formulation maintains effective granuloma concentrations of INH due to the combination of slow carrier-release kinetics, dosing to the site of infection, and gradual distribution of INH from lungs to other tissues. The normalized ratio of granuloma to peripheral AUC is increased 42% and granuloma to plasma AUC is increased 37% (**Figure 4d**), indicating that the inhaled formulation is able to provide additional granuloma exposure while simultaneously reducing toxicity (**Supplementary Figure S3b-d**). Increased relative exposure in the granuloma from an inhaled formulation occurs at a significantly reduced total 2-week dose (**Figure 4a**). Together, these results demonstrate that a suitably designed inhaled formulation of INH can reduce dose frequency, increase sterilizing capability, and reduce toxicity by maintaining suitable concentrations in granulomas for the entire dosing window.

DISCUSSION

Rational development of inhaled antibiotic formulations for treatment of TB necessitates a systems pharmacology approach that simultaneously captures pharmacokinetics, granuloma dynamics, carrier-release dynamics and behavior, and pharmacodynamics. We developed a computational model that tracks these dynamics and used it to understand what controls treatment efficacy and to rationally design inhaled formulations with reduced dosing frequencies.

We predict that an inhaled formulation of INH, dosed every 2 weeks, would have better sterilizing capabilities and reduced toxicity compared with daily oral dose formulations. The antibiotic loading of INH is highly feasible (~30%–50% w/w) and slow release kinetics could be designed by modulating physiochemical properties of carriers such as polymer molecular weight.[21] In contrast, inhaled formulations of RIF, dosed every 2 weeks, have equivalent sterilizing capabilities as daily oral dose formulations, but with early increased toxicity. Additionally, impractical carrier loadings of RIF, exceeding 90% w/w, likely render it a nonviable alternative. Two factors contribute to stable antibiotic concentrations (RIF and INH) in the lungs after inhaled dosing: (1) directly dosing to lungs bypasses the first hepatic pass associated with oral dosing, (2) transport of antibiotics is reversed (antibiotic is released into lungs and absorbs into plasma to be cleared vs. antibiotic absorbing into the plasma, circulating to lungs, and absorbing into lungs). Thus, concentrations of antibiotics in the lungs can be maintained at higher concentrations for extended periods of time as compared to oral dosing.

There has been considerable effort targeting inhaled carriers to macrophages, assuming that increasing intracellular antibiotic concentrations would increase sterilization.[12,13,15–18] Using our model, we predict that targeting carriers to macrophages has limited effects on overall treatment efficacy. This is principally due to discrepancies between *in vitro* settings, where the majority of macrophages are infected and an abundance of carriers are available for phagocytosis, and *in vivo* infection scenarios, where infected macrophages reside in the center of a densely packed granuloma.

Compliance is a long-standing concern for TB treatment. Current oral regimens are lengthy and complex, which contributes to failed treatments.[1] Direct-observed treatment short-course now accompanies most regimens in an attempt to prevent failures, yet successful treatment rates of antibiotic-susceptible TB are only 34%–76%.[47,48] New treatment strategies that reduce dose frequency and alleviate "pill-burdens" could revolutionize treatment compliance. We predict that properly designed inhaled formulations of INH could be promising avenues to accomplish these goals. However, the applicability of inhaled formulations must be taken in context with other antibiotics, as monotherapies are not used for treatment of TB due to development of antibiotic resistance. Furthermore, hosts have multiple granulomas (~3–30), thus success of treatment at the host scale is the collective success of treatment in individual granulomas.[34]

The incidence of both multidrug resistant and extensively drug resistant TB cases is rising.[49] Although inhaled formulations can reduce dosing frequencies, exposing *Mtb* to lengthy periods of low antibiotic concentrations might cause onset of antibiotic-resistance.[1,50] Inhaled formulations of RIF may contribute to increased resistance due to diminishing antibiotic concentrations in granulomas during less-frequent dosing windows (**Figure 3c**). Inhaled formulations of INH could prevent resistance development by reducing cycling between effective and noneffective antibiotic concentrations associated with daily oral dosing. Additionally, faster times to sterilization could reduce the likelihood of resistance mutations (**Figure 4c**). Further work with our systems pharmacology approach is needed to develop an accurate model of antibiotic-resistance to further assess clinical viability of inhaled formulations.

Current treatment strategies for TB rely on antibiotics developed half a century ago, before the advent of systems pharmacology approaches.[1] Herein, we developed a computational approach to design inhaled formulations of RIF and INH for treatment of TB. We found that inhaled formations of INH are promising, yet inhaled formations of RIF are likely ineffective due to toxicity concerns. There has been limited testing of inhaled formulations in humans and NHPs with TB due to high costs and ethical concerns. Our model framework functions as a tool to rapidly assess efficacy of inhaled formulations in a representative model of TB that can be tested in and validated against future *in vivo* data. In addition, this platform can be readily adapted to prototype possible inhaled formulations of "second-line" antibiotics used to treat drug-resistant TB. Second-line antibiotics, such as fluoroquinolones and aminoglycosides, are given for 18–24 months and are highly toxic.[1] The ability to quickly assess which second-line antibiotics would be promising candidates for an inhaled formulation would considerably reduce development time of new treatments. Our unique computational platform, used in parallel with experimental models, provides an integrated approach to improve treatment of TB.

Acknowledgments. We thank Joanne Flynn and the members of her research group for providing the existing experimental measurements of orally dosed antibiotics in the non-human primate model of infection and also for helpful discussions. We thank Paul Wolberg and Joe Waliga for computational assistance.

Author Contributions. N.C., D.K., J.L. wrote the manuscript. N.C., E.P., G.T., D.K., J.L. designed the research and analyzed the data. N.C. performed the simulations.

Conflict of Interest. The authors declare no conflict of interest. This research was supported in part through computational resources and services provided by: National Energy Research Scientific Computing Center, which is supported by the Office of Science of the U.S. Department of Energy under Contract No. DE-AC02-05CH11231; Open Science Grid, which is supported by the National Science Foundation and the U.S. Department of Energy's Office of Science; Advanced Research Computing at the University of Michigan, Ann Arbor. This research was funded by the following NIH grants: R01 EB012579 (D.E.K. and J.J.L.) and R01 HL 110811 (D.E.K. and J.J.L.).

Study Highlights

WHAT IS THE CURRENT KNOWLEDGE ON THE TOPIC?

✓ Inhaled formulations of antibiotics have shown promise in experimental systems, however, a fundamental understanding of the dynamics contributing to increased efficacy remains limited. Thus, there is a need for a system that takes into account simultaneous dynamics of the granuloma, carrier release kinetics, pharmacokinetics, and pharmacodynamics.

WHAT QUESTION DID THIS STUDY ADDRESS?

✓ This study addressed how carrier physiochemical properties and release kinetics (e.g., size, diffusivity, etc.), dosing frequency, and pharmacokinetics control treatment efficacy of inhaled formulations of RIF and INH.

WHAT THIS STUDY ADDS TO OUR KNOWLEDGE

✓ Our platform captures antibiotic dynamics across multiple transport compartments and demonstrates that these dynamics must be considered together when designing inhaled formulations. This allows us to rationally design inhaled formulations to increase efficacy and reduce noncompliance and toxicity issues of existing antibiotics.

HOW THIS MIGHT CHANGE CLINICAL PHARMACOLOGY AND THERAPEUTICS

✓ Our *in silico* approach can help facilitate development of new treatments by quickly assessing the efficacy of inhaled formulations of antibiotics for the treatment of TB.

1. Dartois, V. The path of anti-tuberculosis drugs: from blood to lesions to mycobacterial cells. *Nat. Rev. Microbiol.* **12**, 159–167 (2014).
2. Griffiths, G., Nyström, B., Sable, S.B. & Khuller, G.K. Nanobead-based interventions for the treatment and prevention of tuberculosis. *Nat. Rev. Microbiol.* **8**, 827–834 (2010).
3. O'Garra, A. *et al.* The immune response in tuberculosis. *Annu. Rev. Immunol.* **31**, 475–527 (2013).
4. Global Tuberculosis Report 2013. 1–145 (World Health Organization).
5. Zumla, A., Nahid, P. & Cole, S.T. Advances in the development of new tuberculosis drugs and treatment regimens. *Nat. Rev. Drug Discov.* **12**, 388–404 (2013).
6. Lin, P.L. *et al.* Metronidazole prevents reactivation of latent *Mycobacterium tuberculosis* infection in macaques. *Proc. Natl. Acad. Sci. USA* **109**, 14188–14193 (2012).
7. Flynn, J.L. & Chan, J. Immunology of tuberculosis. *Annu. Rev. Immunol.* **19**, 93–129 (2001).
8. Lin, P.L. *et al.* Sterilization of granulomas is common in active and latent tuberculosis despite within-host variability in bacterial killing. *Nat. Med.* **20**, 75–79 (2014).
9. Lin, P.L. *et al.* Early events in *Mycobacterium tuberculosis* infection in cynomolgus macaques. *Infect. Immun.* **74**, 3790–3803 (2006).
10. Kjellsson, M.C. *et al.* Pharmacokinetic evaluation of the penetration of antituberculosis agents in rabbit pulmonary lesions. *Antimicrob. Agents Chemother.* **56**, 446–457 (2012).
11. Pienaar, E. *et al.* A computational tool integrating host immunity with antibiotic dynamics to study tuberculosis treatment. *J. Theor. Biol.* **367C**, 166–179 (2015).
12. Misra, A. *et al.* Inhaled drug therapy for treatment of tuberculosis. *Tuberculosis (Edinb).* **91**, 71–81 (2011).
13. Muttil, P., Wang, C. & Hickey, A. J. Inhaled drug delivery for tuberculosis therapy. *Pharm. Res.* **26**, 2401–2416 (2009).
14. Sosnik, A., Carcaboso, A.M., Glisoni, R.J., Moretton, M.A. & Chiappetta, D.A. New old challenges in tuberculosis: potentially effective nanotechnologies in drug delivery. *Adv. Drug Deliv. Rev.* **62**, 547–559 (2010).
15. Zhou, H. *et al.* Microparticle-based lung delivery of INH decreases INH metabolism and targets alveolar macrophages. *J. Control. Release* **107**, 288–299 (2005).
16. Hirota, K. *et al.* Optimum conditions for efficient phagocytosis of rifampicin-loaded PLGA microspheres by alveolar macrophages. *J. Control. Release* **119**, 69–76 (2007).
17. Parikh, R., Dalwadi, S., Aboti, P. & Patel, L. Inhaled microparticles of antitubercular antibiotic for in vitro and in vivo alveolar macrophage targeting and activation of phagocytosis. *J. Antibiot. (Tokyo)* 1–8 (2014). doi:10.1038/ja.2014.13
18. Muttil, P. *et al.* Inhalable microparticles containing large payload of anti-tuberculosis drugs. *Eur. J. Pharm. Sci.* **32**, 140–150 (2007).
19. Verma, R.K., Kaur, J., Kumar, K., Yadav, A.B. & Misra, A. Intracellular time course, pharmacokinetics, and biodistribution of isoniazid and rifabutin following pulmonary delivery of inhalable microparticles to mice. *Antimicrob. Agents Chemother.* **52**, 3195–3201 (2008).
20. Yoshida, A. *et al.* Selective delivery of rifampicin incorporated into poly(DL-lactic-co-glycolic) acid microspheres after phagocytotic uptake by alveolar macrophages, and the killing effect against intracellular Mycobacterium bovis Calmette-Guérin. *Microbes Infect.* **8**, 2484–2491 (2006).
21. Makino, K. *et al.* Efficient intracellular delivery of rifampicin to alveolar macrophages using rifampicin-loaded PLGA microspheres: effects of molecular weight and composition of PLGA on release of rifampicin. *Colloids Surf. B. Biointerfaces* **36**, 35–42 (2004).
22. Ain, Q., Sharma, S., Garg, S.K. & Khuller, G.K. Role of poly [DL-lactide-co-glycolide] in development of a sustained oral delivery system for antitubercular drug(s). *Int. J. Pharm.* **239**, 37–46 (2002).
23. Sharma, A., Sharma, S. & Khuller, G.K. Lectin-functionalized poly (lactide-co-glycolide) nanoparticles as oral/aerosolized antitubercular drug carriers for treatment of tuberculosis. *J. Antimicrob. Chemother.* **54**, 761–766 (2004).
24. Kumar Verma, R. *et al.* Partial biodistribution and pharmacokinetics of isoniazid and rifabutin following pulmonary delivery of inhalable microparticles to rhesus macaques. *Mol. Pharm.* **9**, 1011–1016 (2012).
25. Dharmadhikari, A.S. *et al.* Phase I, single-dose, dose-escalating study of inhaled dry powder capreomycin: a new approach to therapy of drug-resistant tuberculosis. *Antimicrob. Agents Chemother.* **57**, 2613–2619 (2013).
26. Pandey, R. *et al.* Poly (DL-lactide-co-glycolide) nanoparticle-based inhalable sustained drug delivery system for experimental tuberculosis. *J. Antimicrob. Chemother.* **52**, 981–986 (2003).
27. Coowanitwong, I., Arya, V., Kulvanich, P. & Hochhaus, G. Slow release formulations of inhaled rifampin. *AAPS J.* **10**, 342–348 (2008).
28. Fallahi-Sichani, M., Flynn, J.L., Linderman, J.J. & Kirschner, D.E. Differential risk of tuberculosis reactivation among anti-TNF therapies is due to drug binding kinetics and permeability. *J. Immunol.* **188**, 3169–3178 (2012).
29. Fallahi-Sichani, M., El-Kebir, M., Marino, S., Kirschner, D.E. & Linderman, J.J. Multi-scale computational modeling reveals a critical role for TNF-α receptor 1 dynamics in tuberculosis granuloma formation. *J. Immunol.* **186**, 3472–3483 (2011).
30. Ray, J.C. J., Flynn, J.L. & Kirschner, D.E. Synergy between individual TNF-dependent functions determines granuloma performance for controlling Mycobacterium tuberculosis infection. *J. Immunol.* **182**, 3706–3717 (2009).
31. Cilfone, N.A., Perry, C.R., Kirschner, D.E. & Linderman, J.J. Multi-scale modeling predicts a balance of tumor necrosis factor-α and interleukin-10 controls the granuloma environment during *Mycobacterium tuberculosis* infection. *PLoS One* **8**, e68680 (2013).
32. Cilfone, N.A. *et al.* Computational modeling predicts IL-10 control of lesion sterilization by balancing early host immunity-mediated antimicrobial responses with caseation during *Mycobacterium tuberculosis* infection. *J. Immunol.* **194**, 664–677 (2015).

33. Kirschner, D.E., Hunt, C.A., Marino, S., Fallahi-Sichani, M. & Linderman, J.J. Tuneable resolution as a systems biology approach for multi-scale, multi-compartment computational models. *Wiley Interdiscip. Rev. Syst. Biol. Med.* **6**, 289–309 (2014).
34. Lin, P.L. *et al.* Quantitative comparison of active and latent tuberculosis in the cynomolgus macaque model. *Infect. Immun.* **77**, 4631–4642 (2009).
35. Tabata, Y. & Ikada, Y. Effect of the size and surface charge of polymer microspheres on their phagocytosis by macrophage. *Biomaterials* **9**, 356–362 (1988).
36. Champion, J.A., Walker, A. & Mitragotri, S. Role of particle size in phagocytosis of polymeric microspheres. *Pharm. Res.* **25**, 1815–1821 (2008).
37. Hasegawa, T. *et al.* Phagocytic activity of alveolar macrophages toward polystyrene latex microspheres and PLGA microspheres loaded with anti-tuberculosis agent. *Colloids Surf. B. Biointerfaces* **60**, 221–228 (2007).
38. Kalluru, R. *et al.* Poly(lactide-co-glycolide)-rifampicin nanoparticles efficiently clear Mycobacterium bovis BCG infection in macrophages and remain membrane-bound in phago-lysosomes. *J. Cell Sci.* **126**, 3043–3054 (2013).
39. Cu, Y. & Saltzman, W.M. Controlled surface modification with poly(ethylene)glycol enhances diffusion of PLGA nanoparticles in human cervical mucus. *Mol. Pharm.* **6**, 173–181 (2010).
40. Siepmann, J. & Siepmann, F. Mathematical modeling of drug delivery. *Int. J. Pharm.* **364**, 328–343 (2008).
41. Kanjickal, D.G. & Lopina, S.T. Modeling of drug release from polymeric delivery systems–a review. *Crit. Rev. Ther. Drug Carrier Syst.* **21**, 345–386 (2004).
42. Arifin, D.Y., Lee, L.Y. & Wang, C.-H. Mathematical modeling and simulation of drug release from microspheres: implications to drug delivery systems. *Adv. Drug Deliv. Rev.* **58**, 1274–1325 (2006).
43. Lin, P.L. *et al.* Radiologic responses in cynomolgous macaques for assessing tuberculosis chemotherapy regimens. *Antimicrob. Agents Chemother.* **57**, 4237–4244 (2013).
44. Marino, S., Hogue, I.B., Ray, C.J. & Kirschner, D.E. A methodology for performing global uncertainty and sensitivity analysis in systems biology. *J. Theor. Biol.* **254**, 178–196 (2008).
45. Musante, C.J. *et al.* Factors affecting the deposition of inhaled porous drug particles. *J. Pharm. Sci.* **91**, 1590–1600 (2002).
46. Yeh, H.-C. & Schum, G.M. Models of human lung airways and their application to inhaled particle deposition. *Bull. Math. Biol.* **42**, 461–480 (1980).
47. Pasipanodya, J. & Gumbo, T. An oracle: antituberculosis pharmacokinetics-pharmacodynamics, clinical correlation, and clinical trial simulations to predict the future. *Antimicrob. Agents Chemother.* **55**, 24–34 (2011).
48. Phillips, L. Infectious disease: TB's revenge. *Nature* **493**, 14–16 (2013).
49. Dheda, K. *et al.* Global control of tuberculosis: from extensively drug-resistant to untreatable tuberculosis. *Lancet Respir. Med.* **2600**, 1–18 (2014).
50. Duncan, K. & Barry, C.E. Prospects for new antitubercular drugs. *Curr. Opin. Microbiol.* **7**, 460–465 (2004).

Supplementary information accompanies this paper on the *CPT: Pharmacometrics & Systems Pharmacology* website (http://www.wileyonlinelibrary.com/psp4)